

# Carbon Nanotubes for Field Emission Applications

W.I.Milne & M.T. Cole  
 Engineering Department,  
 Electrical Engineering Division,  
 University of Cambridge  
 Cambridge

*Abstract*— This paper will cover several applications of a particular type of field emitter- the carbon nanotube (CNT). The growth of CNTs and their optimization for use in various applications including, parallel e-beam lithography, field emission displays and microwave sources, is considered.

Keywords-field emission, carbon nanotubes, electronic applications

## I. INTRODUCTION

Large area electron sources, based on a high packing density of field emission sites, produced on appropriate substrates, have attracted much interest since the early 1970s, when the seminal work of Spindt and co-workers provided the basis of modern vacuum nanoelectronics. Since then there have been several attempts to further optimize field emission sources for a variety of applications such as in high resolution electron microscopy, x-ray sources and in back light units for liquid crystal displays. This presentation will cover the use of a particular type of field emitter- the carbon nanotube (CNT) and will consider their growth and optimization for use in applications including, field emission displays, parallel e-beam lithography and microwave sources.

## II FIELD EMISSION DISPLAYS

In 1968, K R.Shoulders and C.A. Spindt [ see e.g 1 ] were some of the first to envisage the fabrication of a field emission flat panel display based on the use of arrays of microscopically sharp Mo tips. They proposed the use of a number of polycrystalline metal thin film physical vapour deposition and etching techniques in addition to high-resolution photo- and electron beam lithography processes in order to form the necessary arrays of conical emitters, typically on Si or optically transparent substrates [1]. Combined with novel matrix addressing, Shoulders and Spindt had come up with the fundamental elements of the field emission display (FED). FEDs are compact, lightweight and define the image using thousands of simultaneously excited electron beams, rather than only a few slow thermally excited beams (typically three), as in the case of the more traditional cathode ray tube (CRT). In an FED, an extraction potential is selectively applied onto bus-like electrodes to address the individual sub-pixels thereby applying a local potential

between the sharp emitting structures and the extraction anode. This induces electrons to be liberated from the electron dense emitter, in a quantum mechanical tunneling process known as ‘field emission’. These excited electrons are then accelerated by the field gradient and are focused, typically by a gate electrode, toward the appropriate phosphor that comprises a single pixel. Each pixel is made up of a red, green or blue sub-pixel and is of the order of 50  $\mu\text{m}$  in size. The incident electron beam excites the RGB phosphors to form the image which is common to both CRTs and FEDs. Other colours are produced by mixing the emission from the RGB phosphors by controllable exciting multiple phosphors simultaneously- see Fig. 1 [adapted from 2-4]. For display applications current densities of  $\sim 5\text{mA}\cdot\text{cm}^2$  are required. CNTs are ideal candidates for field emission applications as they have an exceptionally high aspect ratio, high conductivities, are resistant to electromigration and are exceptionally robust at high temperatures and typically aggressive chemical environments. CNT based FEDs have been produced by various companies in the Far East but are, as yet, not commercially available.

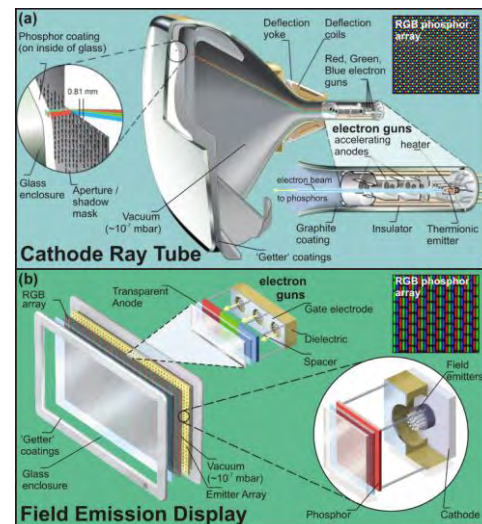


Figure 1. Comparison between CRT and FED

## II. PARALLEL ELECTRON BEAM LITHOGRAPHY

Electron beam lithography is a type of maskless lithography that has found wide usage in the manufacture of high resolution photomasks for photolithography and in low-volume production of semiconductor components, as well as being extensively used in R&D facilities worldwide. However, electron beam lithography offers only a limited throughput due to its serial nature, i.e., the very long time it takes to expose an entire silicon wafer or mask. To overcome this problem parallel e-beam lithography has been investigated. The feasibility of this approach has been demonstrated by Chang *et al.* [5] and Muray *et al.* [6] using an array of four miniature ( $2 \times 2$  cm) electron-beam columns.

We have investigated the feasibility of utilising CNTs for parallel e-beam lithography, with the initial aim of demonstrating the concept with 32 micro-guns [8]. The long term ambitious objective was to achieve high throughput maskless direct writing capability with an array of upto 1 million micro-guns. Even if e-beam lithography does not meet the requirements for mass production of integrated circuits' in the near future, parallel e-beam lithography will still ultimately find itself suitably poised for low cost photomask fabrication (since low throughput single e-beam systems are currently used for manufacturing photomasks) and economical low volume maskless prototype integrated circuit fabrication (since a set of photomasks for current CMOS costs  $\sim 2$  million Euros).

In our approach, scanning is performed in tandem with a control system to determine the required pixels to be exposed in any given pattern. This fixed-focus/fixed-beam position approach has the advantage that the lenses are simpler to design and integrate as it eliminates typical aberrations associated with beam deflection. Thus, if the micro-guns have a pitch of  $100 \mu\text{m}$  (figure 2) the writing time for the entire mask in parallel would be the time to scan the  $100 \mu\text{m} \times 100 \mu\text{m}$  field, which is of the order of 1–5 minutes.

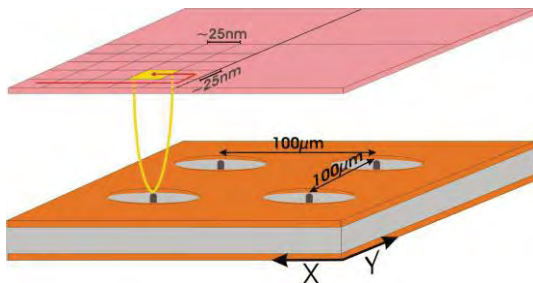


Figure 2. Schematic of CNT based parallel e-Beam Lithography

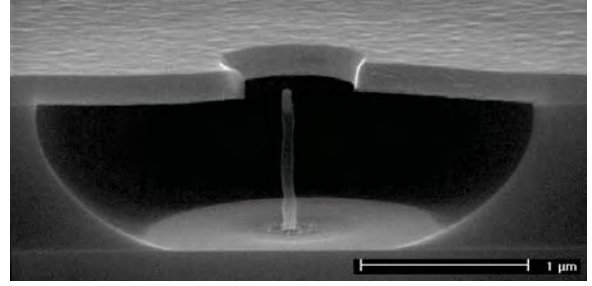


Figure 3. An individual CNT within a gated structure

The most critical parameter for obtaining high resolution is the alignment between the CNT and the extraction gate aperture — these elements constitute the so-called ‘micro-cathode’. This requirement led to the development of a micro-cathode fabrication process in which the CNT emitter and extraction gate are self-aligned. Figure 3 shows a fabricated emitter in cross-section where the CNTs are deposited using a plasma enhance chemical vapour deposition (PE-CVD) process as described in detail elsewhere.[7] Using a  $2 \mu\text{m}$  gate aperture, multiple tubes are produced in each but when high resolution lithography is used to produce catalyst dots approximately 100 nm in diameter then single tubes are produced in each aperture (Figure 3). The field emission behaviour from an array of such micro-guns has been investigated. For an emitter formed from  $100 \times 100$  CNTs the emitted current (reaching the anode) is  $10 \mu\text{A}$  (equivalent to  $\sim 1$  nA per emitter)[8].

## III. MICROWAVE SOURCES

Most long range telecommunication systems are based upon microwave links. In order to satisfy present power (tens of Watts) and bandwidth requirements (30 GHz), satellites employ travelling wave tubes (TWT's) based on thermionic cathodes. However TWTs are bulky and consume large proportions of the valuable space and weight budget in a satellite. Thus any miniaturization of the TWTs would lead to rather significant cost savings in a satellite launch, and indeed aid the implementation of micro-satellites. Solid state devices cannot be used in this high frequency, high bandwidth regime because the maximum power attained by solid state devices today at 30 GHz is  $\sim 1$  W. Therefore the most effective way to reduce the size of a TWT is *via* direct temporal modulation of the e-beam, for example, in a triode configuration. Cold cathodes with the ability of being modulated at 30 GHz do not presently exist. Current cold cathode technology suffers because it is based upon integrated grid systems where the spacing between the cathode and grid is filled with an insulator (typically  $\text{SiO}_2$  or  $\text{Al}_2\text{O}_3$ ), which leads to unavoidably high capacitance. Hence they cannot be directly modulated at GHz frequencies and can only provide the primary (dc) beam.

In the case of CNT arrays, this modulating grid is not integrated and can be located at an extended distance of  $10\text{--}100 \mu\text{m}$  from the emitters where the space between emitter and grid is evacuated ( $10^{-6}$  mbar) with a consequent reduction in

grid/cathode capacitance of the order of 20–50 times, therefore allowing for high frequency operation. A schematic of such an amplifier is shown in Figure 4.

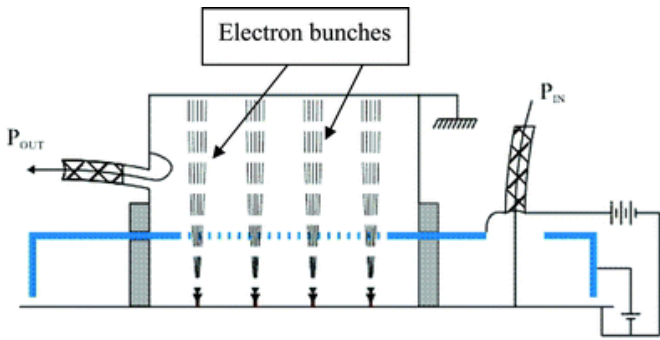


Figure 4. Schematic of CNT based vacuum microwave amplifier [8]

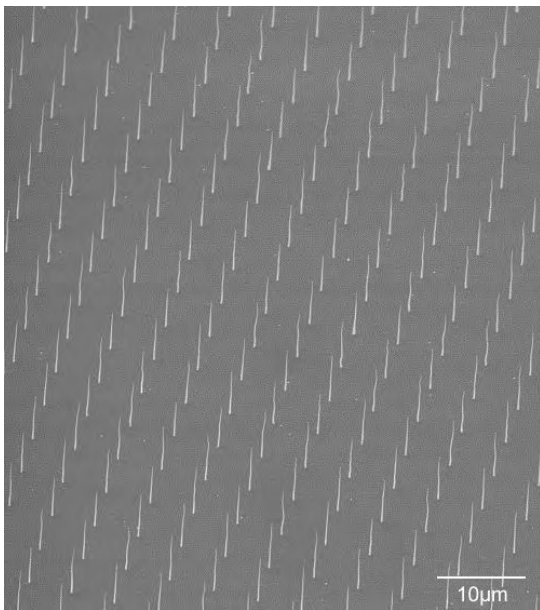


Figure 5. Array of MWCNTs with  $\sigma$  tip dia (~4.1%) and  $\sigma$  height (~6.3%)

In order to be commercially viable and truly competitive with thermionic cathodes for this application, CNT cathodes must deliver current densities in the range 1–2 A/cm<sup>2</sup>. This can only be achieved by controlling the uniformity in height and diameter of the CNTs by understanding their detailed deposition characteristics. Indeed, various CNT types can be grown. By way of an example, figure 5 shows an emitter formed from nominally metallic multi-walled carbon nanotubes. We have demonstrated operation of this system at 1.5 GHz using various radio frequency-input powers to generate different macroscopic electric fields at the apex of carbon-nanotube emitters. A spectrum analyser attached to the output antenna confirmed the presence of the fundamental 1.5-GHz peak in the cavity. Here, cathodes were operated at 1 mA

and 1.5 GHz for 40 h without degradation or a decrease in current output (within the measurement error of 5%). With an applied radiofrequency electric field of 29 MV/m, the output at the anode reaches 3.2 mA, with an average current density of 1.3 A/cm<sup>2</sup>. This corresponds to a peak current of 30 mA and a current density of 12 A/cm<sup>2</sup> in the output waveform [9]. More recently we have demonstrated modulation at 32 GHz with a 1.4 A/cm<sup>2</sup> peak current density from an 82% modulation [9]. In this work, a high cathode–grid spacing (100  $\mu$ m) was used and the applied field was modulated using a resonant cavity. With this configuration, the cathode–grid capacitance was extremely low making it compatible with very high frequency operation. However, the consequence of using a resonant cavity is that the modulated electron source can only be used in narrow bandwidth amplifiers. In order to circumvent this Thales developed a CNT-based optically controlled field emission cathode [9,10]. Here, as opposed to the cathodes described above, the applied electric field is constant. The modulation of the emitted current is obtained through optical excitation. Such devices are thus compatible with high frequency and very large bandwidth operation is possible [10]. Using this new photocathode concept, the first CNT-based photocathode using Si p–i–n photodiodes and MWCNT bundles has been fabricated.

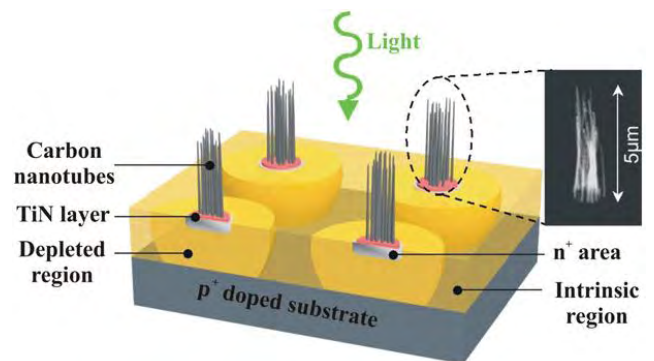


Figure 6. Schematic view of the new MWCNT based photocathode [10].

This photocathode consists of an array of MWCNTs in which each MWCNT is electrically connected to an  $n^+$  doped area defined in an intrinsic layer grown on a  $p^+$  doped semiconducting substrate (Figure 6). Due to the localization of the  $n^+$  areas, the p–i–n diodes are independent of each other. Under an applied field, the MWCNTs emit and the diodes are reversely biased. A voltage drop ( $\Delta V$ ) appears across the diodes, mainly in depletion regions that extend under each  $n^+$  area. Upon illumination by photons, with energy exceeding the band gap of the semiconductor, electron–hole pairs are generated in or near to the depletion region. The carriers are then swept across the depletion region by the electric field and electrons are subsequently emitted by the MWCNTs. When the optical excitation is turned off, the diode current becomes very small (equal to the leakage current of the diode). The electrons previously accumulated at the MWCNT apex are still field emitted through the available electron population to be emitted

is substantially reduced. Thus the emitted current decreases and adjusts to the diode leakage current. During this process, as the emission current has been higher than the diode current, the MWCNTs have become positively biased compared to the substrate. The voltage drop within the diode ( $\Delta V$ ) has attained its maximum value. It is of prime importance to estimate this value and to design the photocathode in order to avoid diode breakdown. Using such device, for the first time, optical modulation of the emission current from carbon nanotubes by pulsing the laser source as shown in figure 6 and 7 has been demonstrated.

As shown in figure 7(a), the device was tested under ultra-high vacuum ( $10^{-9}$  mbar) in a triode configuration with a cathode-grid distance of 100  $\mu$ m. The anode consists of a glass plate coated with a thin indium tin oxide (ITO) layer. The photocathode is then illuminated through this transparent

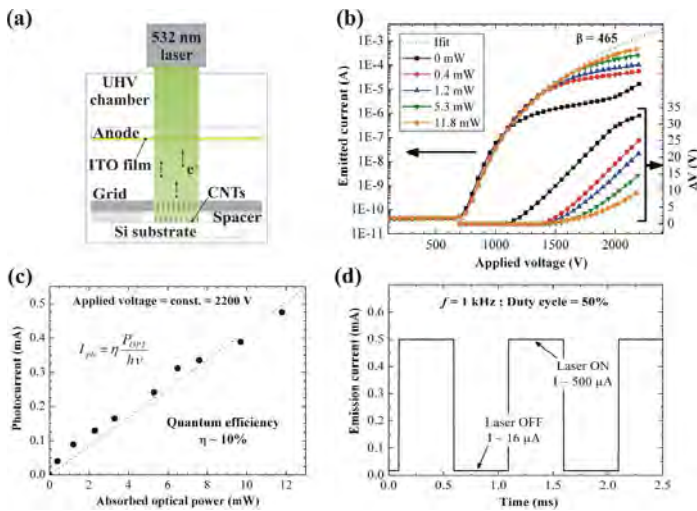


Figure 7. Schematics of the experimental setup with the cathode-grid assembly (spacer thickness = 100  $\mu$ m), the transparent and conductive anode, and the 532 nm laser [10].

and conductive anode, using the optical source. To create free carriers in the intrinsic Si, photons of energy roughly equal or greater than the band gap (1.12 eV for silicon, corresponding to a wavelength of less than 1100 nm) have to be absorbed. A 532 nm green laser was consequently employed as the optical source. Using a controlled laser-pulse at this frequency this photocathode delivers 0.5 mA with an internal quantum efficiency of 10% and an  $I_{ON}/I_{OFF}$  ratio of 30.

In figure 7 (b), the emitted current of the photocathode is plotted as a function of the cathode-grid applied voltage and for absorbed optical powers  $P_{OPT}$  ranging from 0 to 11.8 mW (left axis). The black curve represents the non-illuminated photocathode emission current, and the remaining coloured curves represent the photocathode emission current for various absorbed optical powers ( $P_{OPT}$ ). The absorbed optical powers were determined taking into account the transparency of the ITO/glass, the grid and the reflection from the Si surface. The dashed curve is the Fowler-Nordheim (FN) fit for the

experimental curves in the low emission current region, i.e. where the effect of the limiting current of the p-i-n diode is negligible. At higher voltages, the curves deviate from the FN law and exhibit different saturations, corresponding to the different absorbed optical powers. In this saturation regime, a voltage drop appears across the p-i-n diode and limits the emission current because the p-i-n photocurrent is insufficient to feed the emission, even under high illumination.

The first demonstration was performed at relatively low frequency as shown in fig. 7(d). The device was operated for 2 months at 0.5 mA without any observable degradation in current. This is due to the optical stability of p-i-n diodes and excellent emission stability of the MWCNTs. By incorporating high frequency p-i-n photodiodes (e.g. GaInAs photodiodes) into the structure and driving them with 1.55  $\mu$ m telecommunication lasers, photocathodes operating in the 10-30 GHz range can be envisaged.

#### IV CONCLUSIONS

CNTs are ideal candidates for field emitters as they have an exceptionally high aspect ratio, high conductivity, are resistant to electro-migration and are robust at elevated temperatures and chemically aggressive environments. Here we have described the use of CNTs in a selection of electronic applications including field emission displays, electron beam lithography and travelling wave tubes.

#### V ACKNOWLEDGEMENTS

This work has been carried out in collaboration with various industrial laboratories and academic groups. Firstly the authors' thank the various PhD students and post docs who have contributed to the work especially Dr K. B. K. Teo, Dr M. Mann and Dr. Y. Zhang. Special thanks are also extended to Dr P. Legagneux and co-workers from Thales with whom we collaborated on both the e-beam lithography and microwave amplifier projects.

#### IV. REFERENCES

- [1] Shoulders, K. R. Microelectronics using electron-beam-activated machining techniques, *Advances in Computers*, 1968
- [2] Cole, M. T., Milne, W. I. and Nakamoto, M. [Handbook of digital imaging - field emission displays and surface-conduction electron-emitter displays eds. Kriss, M., (John Wiley & Sons, Ltd., (2012).
- [3] G.A.J. Amaratunga, "Watching the nanotube, *IEEE Spectr.*, 40, 28-32 (2003).
- [4] Online, E. B. "Cathode-ray tube (crt) <http://www.Britannica.Com/ebchecked/topic/99774/cathode-ray-tube-crt>," 2012
- [5] T. H. P. Chang, D. P. Kern and L. P. Murray, *J. Vac. Sci. Technol., B*, 1992, **10**, 2743
- [6] L. P. Muray, J. P. Spallas, C. Stebler, K. Lee, M. Mankos, Y. Hsu, M. Gmur and T. H. P. Chang, *J. Vac. Sci. Technol., B*, 2000, **18**, 3099
- [7] M. Chhowalla et al., *J. Appl Phys* 90, 10, 5308-5317, 2001
- [8] W.I.Milne et al *J. Mater. Chem.*, 2004,**14**, 933-943
- [9] P.Legagneux et al IVEC 2009.
- [10] L.Hudanski et al, *Nanotechnology*, 19,10, 2008